Original Paper

Mechanical properties of sheet glass at high pressure during indentation experiments

Holger Meinhard, Wolfgang Fränzel and Peter Grau

Fachbereich Physik, Martin-Luther-Universität Halle-Wittenberg, Halle/Saale (Germany)

Viscous flow is responsible for permanent deformation of glasses above the transformation temperature (T_g). The results of macroscopic indentation experiments (maximum loading forces $F_{max} \geq 2$ N) with sharp indenters (Vickers or Berkovich pyramids) demonstrate this property by crack-free indents at $T \geq T_g$. But it is also possible to make crack-free indents at room temperature (RT), well below T_g, if the load, the contact area and the deformation rate, respectively, are small enough, which is consistent with glass as a supercooled liquid but inconsistent with glass as a well-known ideally brittle material at RT. The mechanisms of this permanent deformation of glasses by indentation near RT have not been understood completely up to now. For the analysis of the macroscopic indentation experiments with Vickers pyramids and spherical indenters, respectively, a viscoelastic deformation behaviour is assumed for the complete temperature range from RT to T_g. Therefore the rheological analysis of all experiments were performed with the help of a simple Maxwell model. The results of Vickers indentation experiments were compared with cylinder compression experiments and ball indentation experiments which were analysed by the same rheological principles.

Mechanische Eigenschaften von Flachglas unter hohen Drücken bei Indentereindruck-Experimenten

Für Temperaturen oberhalb der Transformationstemperatur (T_g) ist das viskose Fließen als Ursache für die permanente Glasverformung unbestritten. Bei makroskopischen Eindruckexperimenten (Belastungskräfte $F_{max} \geq 2$ N) mit spitzen Indentern (z.B. Vickers- oder Berkovich-Pyramiden) äußert sich dies bei $T \geq T_g$ durch die Rißfreiheit der bleibenden Eindrücke. Bei sehr kleinen Belastungen, Kontaktflächen bzw. Deformationsgeschwindigkeiten ist jedoch die Erzeugung bleibender und auch rißfreier Eindrücke auch bei Raumtemperatur (RT), also weit unterhalb von T_g, möglich. Dies ist verständlich, wenn Glas als unterkühlte Flüssigkeit angesehen wird, jedoch unverständlich, wenn es, wie allgemein üblich, bei diesen Temperaturen als ideal sprödes Material betrachtet wird. Der dieser Verformung zugrundeliegende Mechanismus wird bisher nicht vollständig verstanden. Bei der Analyse von makroskopischen Eindruckexperimenten mit Vickerspyramiden bzw. Kugelindentern wird, zunächst hypothetisch, von viskoelastischem Deformationsverhalten im gesamten Temperaturbereich von RT bis T_g ausgegangen. Für die rheologische Auswertung aller Experimente wurde daher ein einfaches Maxwell-Modell verwendet. Die Ergebnisse der Vickers-Eindruckexperimente werden mit denen von Zylinderstauchversuchen und Kugeleindruckexperimenten verglichen, welche nach denselben rheologischen Prinzipien ausgewertet wurden.

1. Introduction

With a nanoindentation technique it is possible to make permanent indents on glasses even at room temperature (RT). It could be shown by imaging with an atomic force microscope (AFM) that these indents can be without cracks. In figure 1 an AFM image of an indent on float glass, made with a Berkovich indenter (maximum loading force $F_{max} = 300$ mN), is shown exemplarily [1]. In 1933 Tammann [2] used the criterion of non-crack formation to define the transformation temperature T_g by conventional indentation experiments. The indents were performed during increasing temperature step by step. That temperature was identified as T_g of the glass from which on the indents were without cracks. Because the viscous flow is responsible for permanent deformation of glasses above T_g, the deformation process of glasses without crack formation during indentation at RT is considered as an indicator for viscous flow behaviour in Tammann's view. Irrespectively, viscosity values η from 10^{20} Pa s [3] to 10^{40} Pa s [4] at RT were proposed for glasses. That means the Maxwell relaxation time τ, defined by

$$\tau = \frac{\eta}{E_\infty} \tag{1}$$

where E_∞ is the unrelaxed elastic modulus, which amounts to 10^9 s and 10^{29} s, and is incompatible with

Received 23 August 2001.

Presented in German at the 74th Annual Meeting of the German Society of Glass Technology (DGG) in Ulm (Germany) on 30 May 2000.

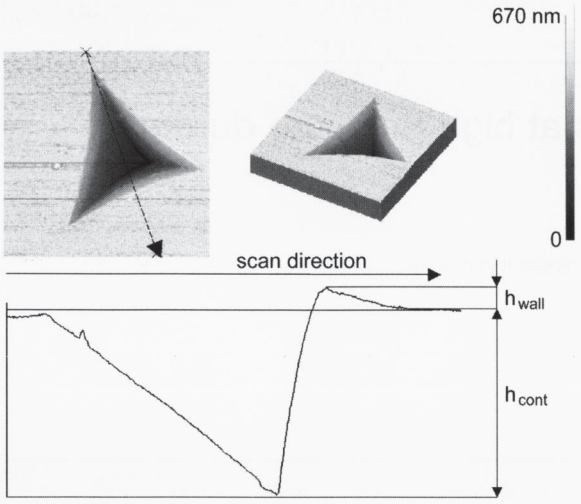

Figure 1. Atomic force microscopy (AFM) image of an indent carried out with a Berkovich indenter on commercial float glass at room temperature (top: height mode, bottom: single scan line) (from [1]).

the duration of indentation experiments of 100 s. One possible explanation of this inconsistency is the assumption that the viscosity is reduced substantially under the special stress conditions of indentation experiments. The stresses in the small volume under the indenter tip, represented by the hardness number, are many times higher than it is reachable by uniaxial compression or tension experiments. Another explanation is the input of mechanical energy and hence an increase in temperature and a decrease in viscosity. A rough adiabatic estimation yields sufficiently high temperatures [5].

In [6] an experimental program was introduced to verify the viscosity hypothesis by different methods. In the temperature range from 400 °C to T_g contact experiments were carried out which in principle, work like penetration viscometers (cylinder compression experiments, indentation experiments with spherical indenters). In this paper the gap in measurements from RT to 400 °C is closed down for indentation experiments with spherical indenters. Furthermore, indentation experiments with a sharp indenter (Vickers pyramid) were realized in the complete temperature range from RT to T_g to vary the pressure and stress conditions. All experiments were analysed using the same rheological principles. Using a three-parameter Zener-Maxwell standard model the nonlinear least squares fitting procedure determined the elastic parameter $E_H \approx 0$ of the single Hookean element for all measurements at any used temperature [6]. That means glass behaves like a Maxwellian liquid in deformation experiments. Therefore the indentation experiments with Vickers indenters where analysed by the Maxwell model which had to be modified theoretically with respect to the different contact conditions compared to cylinder compression experiments and indentation experiments with spherical indenters.

2. Theoretical

Using a simple Maxwell model to describe a pure viscoelastic material yields the following differential equation:

$$\dot{\sigma} + \frac{E_M}{\eta}\sigma = E_M \dot{\varepsilon} \tag{2}$$

where σ is the stress, ε is the strain, E_M is the elastic parameter of the Hookean element, η is the viscosity parameter of the Newtonian element and the dotted symbols stand for the rates of the corresponding quantities. For the loading part with $\dot{\varepsilon} = \dot{\varepsilon}_c = \text{const}$ and $\varepsilon = \dot{\varepsilon}_c t$ the solution of equation (2) is:

$$\sigma(t) = \dot{\varepsilon}_c \eta \left[1 - \exp\left(-\frac{E_M}{\eta} t\right)\right], \quad t \le t_f \tag{3}$$

where t_f is the final time of the loading part. For the relaxation experiment with $\varepsilon = \varepsilon(t = t_f) = \varepsilon_f = \text{const}$ yields:

$$\sigma(t) = \sigma_f \exp\left(-\frac{E_M}{\eta}(t - t_f)\right), \quad t > t_f \tag{4}$$

with $\sigma_f = \sigma(t = t_f)$. The equations (3) and (4) were used in [6] to analyse the uniaxial cylinder compression experiments.

The relation between the loading force F and the indentation depth h_{el} for pure elastic deformation by indentation is given in [7 and 8]:

$$F = C_G E^* h_{el}^2 \approx C_G \frac{E}{1 - \nu^2} h_{el}^2 \tag{5}$$

where $C_G = 2.22$ is the numerical constant of the Vickers pyramid and E^* is the reduced elastic modulus resulting from $1/E^* = (1 - \nu^2)/E + (1 - \nu_i^2)/E_i$. Here E, ν and E_i, ν_i are the elastic modulus and the Poisson ratio of the sample and the indenter, respectively. For $E_i \gg E$ it is approximately $E^* \approx E/(1 - \nu^2)$.

To describe the deformation behaviour of viscoelastic materials during indentation experiments, in [9] a solution to this problem is proposed by replacing the elastic constants in the solution to the associated elastic problem by viscoelastic functions $E \leftrightarrow \{m_v \cdot \Psi(t)\}$, where m_v is the geometric constant to verify the special kind of the deformation process ($m_v = 1$ for shear and $m_v = 3$ for tensile experiments [10]). To analyse all types of deformation experiments by the same rheological model the function $\psi(t)$ was derived from the Maxwell model in accordance with equation (3) for the loading part:

$$\psi(t) = \eta\,\dot{\varepsilon}_c\left[1 - \exp\left(-\frac{E_M}{\eta}\,t\right)\right]. \tag{6}$$

Using $\dot{\varepsilon}_c = \dot{h}/h$, the time-dependence for the loading part of deformation by Vickers indentation with fixed indentation rate $\dot{h} = \dot{h}_c$= const is given by:

$$F(t) = \Gamma_v\,\dot{h}_c^2\left[\eta\left(1 - \exp\left(-\frac{E_M}{\eta}\,t\right)\right)t\right], \quad t \le t_f \tag{7}$$

with

$$\Gamma_v = \frac{C_G\,m_v}{1 - \nu^2}. \tag{8}$$

Using the same principle for the relaxation part (see equation (4), but with $\dot{h}_c = 0$ and $h(t = t_f) = h_f$ = const) yields for the time-dependence of the load:

$$F(t) = F_f \exp\left(-\frac{E_M}{\eta}\,(t - t_f)\right), \quad t > t_f \tag{9}$$

where $F(t = t_f) = F_f$ is the loading force at the starting time of the relaxation experiment. It is remarkable that the method of replacing the elastic constants by viscoelastic functions leads for spherical indenters to exactly the same results but with another numerical constant Γ_s [6].

To estimate the mean contact pressure during indentation with spherical and Vickers indenters, respectively, the hardness numbers were used. For dynamic Vickers indentation the definition of the Martens Hardness number HM [11] was used:

$$HM = \frac{F}{c\,h^2} \tag{10}$$

where c is the geometric constant of the pyramidal indenter (c = 26.43 for Vickers pyramid). Different from the so-called plastic hardness, where only the contact depth is used for the calculation of the hardness number, the Martens Hardness includes both the elastic and the inelastic part of indentation depth. A corresponding hardness number to HM for spherical indenters is

$$H_s = \frac{F}{2\,\pi\,R\,h} \tag{11}$$

where R is the radius of the sphere.

3. Experimental

All experiments were performed on commercial sheet glass (T_g = 535 °C, composition (in mol%): 71 SiO_2, 15 Na_2O, 6.6 CaO, 4 MgO, 2 Al_2O_3, 0.9 K_2O, 0.4 SO_3, 0.1 Fe_2O_3). The indentation experiments with spherical and pyramidal indenters were performed on (20 x 20 x 7.5) mm^3 plates. After cutting the samples were homogenized at 535 °C for over 3 h to anneal the mechanical and thermal stresses. The samples were cooled down to RT at rates of 1 K/min. Before starting the deformation experiments at elevated temperatures the samples were stored once more for one hour at the deformation temperature.

For the indentation experiments the servo hydraulic material testing system MTS® 810 (MTS Systems Corporation, Minneapolis, MN (USA)) was used. The different temperature conditions in a range from RT to 540 °C were realized by an additional home-built equipment [6]. A special feature of this equipment is the possibility to measure the real time-dependences of the temperature $T(t)$ and the deformation parameter $F(t)$ and $h(t)$, respectively, directly and simultaneously at the sample during deformation experiment. In this way it was possible to control the deformation process by the real indentation depth. For that reason it was not necessary to know a correction function to eliminate the part of deformation of the testing system as this was done by Brückner et al. [12]. The accuracy of temperature registration of the sample was better than 1 K. A heating of the specimens during the deformation process was not detectable in the 1 K sensitivity limit.

The home-built equipment for temperature-dependent deformation experiments is constructed so that it is very easy to insert indenters of different geometrical shapes. For this work a Vickers and a spherical indenter made of tungsten carbide (Young's modulus E = 830 GPa) were used. This material is qualified for indentation experiments up to 600 °C because of high temperature stability. To obtain consistency for the various indentation tests, an experiment was performed composed of the two parts of deformation according to the uniaxial cylinder compression and to the spherical indentation tests of the former work [6]. After loading parts at a constant rate of indentation depth ($\dot{h}_c$ = 0.1667 µm/s) up to a maximum load $F_{max} = F(t = t_f) = F_f$ (F_f = 100 N for Vickers and F_f = 400 N for spherical indentation), a holding part with constant indentation depth ($h(t = t_f) = h_f$ = const) followed with the same duration of the temperature-dependent loading time for numerical equivalence. From the data of these experiments the rheological parameters were calculated by equations (7) and (9). These experiments were performed in the temperature range from RT (35 °C) to 540 °C (T_g = 535 °C).

In addition to [6], indentation experiments with spherical indenters (R = 1.5 mm) were performed in the same temperature range and with the same constant rate of indentation depth. It could be shown in [6] that two indentation rates which were differing in one order of magnitude yield no significant differences of values for rheological parameters in accordance with the theoretical expectancy. In this case only one indentation rate was

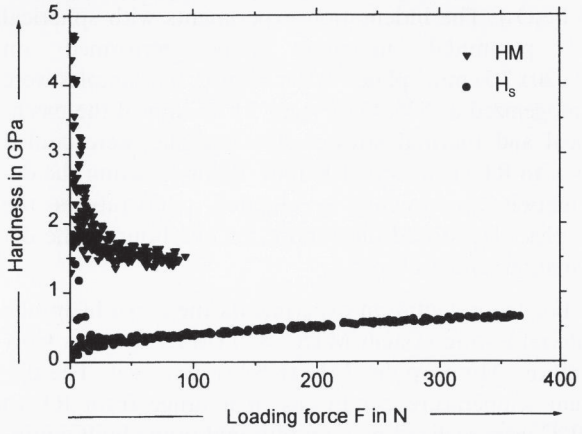

Figure 2. Hardness profiles of the loading process of a single Vickers indentation test (*HM*, equation (12)) and a single spherical indentation test (H_s, equation (13)) at 520 °C.

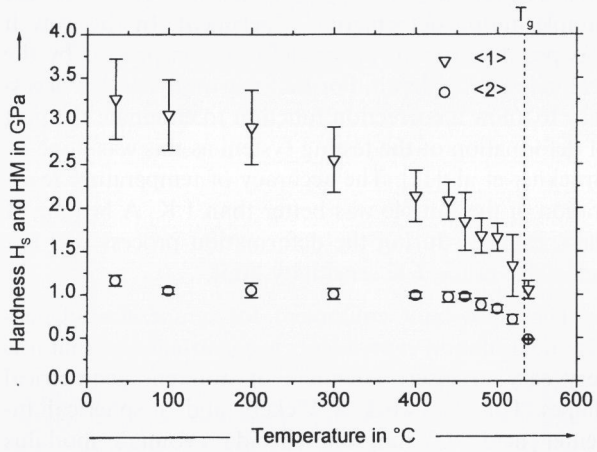

Figure 3. Dependence of hardness numbers *HM* (<1>) and H_s (<2>) on the test temperature.

used and is discussed in this work. For each temperature four single indents were made with both indenters. According to [6] single Vickers indents performed at typical temperatures were investigated by topographical profiling after unloading with a HOMMEL-Tester T2000 (Hommelwerke GmbH, VS-Schwenningen, Germany).

4. Results and discussion

4.1 Hardness numbers *HM* and H_s

In figure 2 the hardness profiles (indentation force-dependence of the hardness numbers) of the loading process with respect to equations (10) and (11) are shown for single indentation experiments at 520 °C with Vickers and spherical indenters, respectively. The hardness numbers *HM* of the Vickers indentation experiment are significantly higher than the hardness numbers of spherical indentation H_S. The extrapolation of the load-dependent *HM* values (indentation size effect) to the maximum load of spherical indentation (F_{max} = 400 N) also yield higher *HM* numbers. In figure 3 the mean values

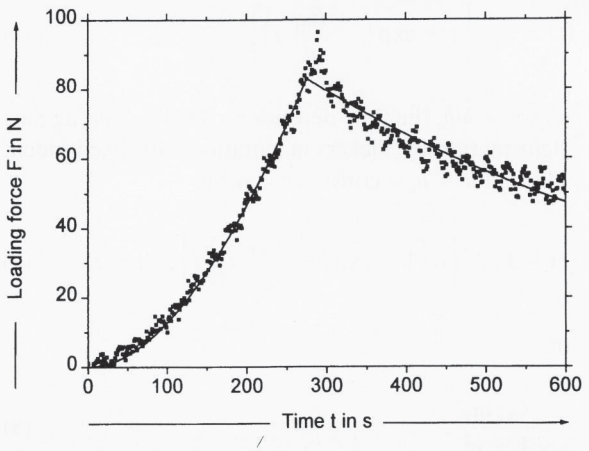

Figure 4. Measuring points and the fitting curve in accordance with equations (9) and (11) of a single Vickers indentation experiment with constant indentation rate and relaxation at 520 °C.

and the corresponding standard deviation of the hardness numbers for the maximum forces *HM* (<1>, F_{max} = 100 N) and H_S (<2>, F_{max} = 400 N) of four single measurements are shown as a function of the test temperature. The hardness numbers decrease with increasing temperatures as expected. It also visible that *HM* is significantly higher than H_S at each testing temperature. That implicates higher stresses during Vickers indentation experiments.

4.2 Viscosity parameter η

In figure 4 the measuring points of the load-time dependence of a single Vickers indentation experiment (T = 520 °C), once more with a loading part ($\dot{h} = \dot{h}_c$ = const = 0.1667 µm/s) and a relaxation part ($h(t = t_f) = h_f$ = const), is shown to exemplify tests which were analysed by rheological principles in accordance with equations (7) and (9). The visible straggling of the data points is caused by the vibration of the hydraulic measurement system. The first step of analysis was the calculation of the pre-factors Γ_v and Γ_s of the solution $F(t)$ (see equation (8)) for deformation by Vickers- and spherical indenters, respectively. Here the measuring points of the four single indentation experiments at RT (35 °C) were fitted according to equations (7) and (9) with fixed parameter E_M and varying parameters Γ and η. The elastic parameter was fixed to E_M = 73.3 GPa which is the value of the Young's modulus at RT of the used sheet glass. The calculated mean values of the pre-factors and the corresponding standard deviations are $\Gamma_v = 1.2 \pm 0.2$ and $\Gamma_s = 4.2 \pm 0.6$. For the following calculation of the rheological parameters E_M and η by a nonlinear least squares fit procedure in accordance with equations (7) and (9) for all temperatures the pre-factors Γ_s and Γ_v were fixed to the mean values, neglecting the temperature-dependence of the Poisson ratio ν. This fit pro-

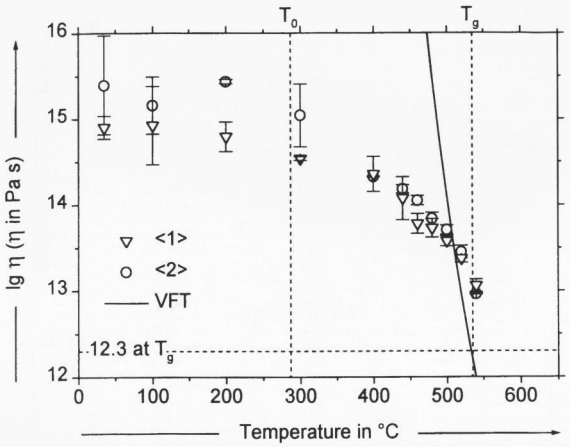

Figure 5. Viscosity parameters of Vickers indentation experiments (<1>, Γ_v = 1.2) and spherical indentation (<2>, Γ_s = 4.2) analysed by equations (9) and (11) as a function of temperature. The constants of the Vogel-Fulcher-Tammann relation (VFT) were fitted by the experimental results of the cylinder compression experiments in [6].

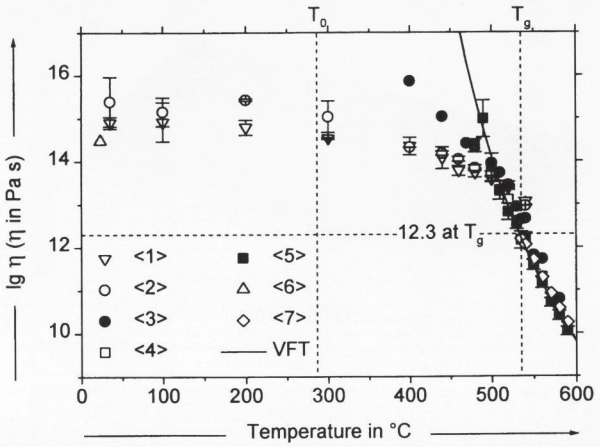

Figure 6. Viscosity parameters of Vickers indentation experiments (<1>, Γ_v = 1.2) and spherical indentation experiments (<2>, Γ_s = 4.2) analysed by equations (9) and (11), indentation creep experiments with the spherical indenter analysed like the penetration viscometer method (<3>, from [6]), cylinder compression experiments analysed by rheological principles (<4>, from [6]), cylinder compression experiments analysed like parallel plate viscometer (<5>, from [6]), nanoindentation experiments (<6>, from [6]) and beam-in-bending experiments (<7>, from [6]) versus temperature. The constants of the Vogel-Fulcher-Tammann relation (VFT) were fitted by the experimental results of the cylinder compression experiments (<4> and <5>, from [6]).

cedure was performed with the complete file of measuring points. That means both parts of the deformation process, loading and relaxation, were described consistently by the same set of rheological parameters.

The results of the two types of indentation experiments (Vickers and spherical indenter) with respect to equations (7) and (9) are shown in figure 5. The calculated viscosity values at T_g are one order of magnitude greater than the value per definition $\eta(T_g) = 10^{12.3}$ Pa s. The following reasons are possible: The determination of the pre-factor Γ (see equations (7) and (9)) is too inaccurate for instance because the temperature-dependence of the Poisson ratio is neglected. It is also possible that the Maxwell model with a single Maxwell time is too simple to describe the viscoelastic behaviour of glass during indentation experiments. It is interesting that the calculated viscosity values of Vickers indentation experiments are smaller than the values of spherical indentation in tendency. With respect to the higher stresses during Vickers indentation (see figure 3) this fact can be a first hint to the stress-dependency of the viscosity, at least under the conditions of contact experiments. This result indicates a decrease of viscosity with increasing stress and pressure, respectively.

In figure 6 the viscosity parameters obtained from the different kinds of deformation experiments and analysis methods are shown together with the relation of Vogel, Fulcher, and Tammann (VFT) [13 to 15]:

$$\lg \eta = A + \frac{B}{T - T_0} \tag{12}$$

where η is the viscosity (in Pa s) at the temperature T, A and B are constants, and T_0 is the so-called Vogel temperature. The values were fitted to A = 0.652, B = 2868.7 °C, and T_0 = 286.5 °C by the results of cylinder compression experiments in principle of a parallel plate viscometer [6]. The same qualitative temperature-dependence of the viscosity was found in [16] by experimental investigations with a flexure pendulum equipment. It is remarkable that the values for the viscosity, calculated from indentation experiments by rheological principles,

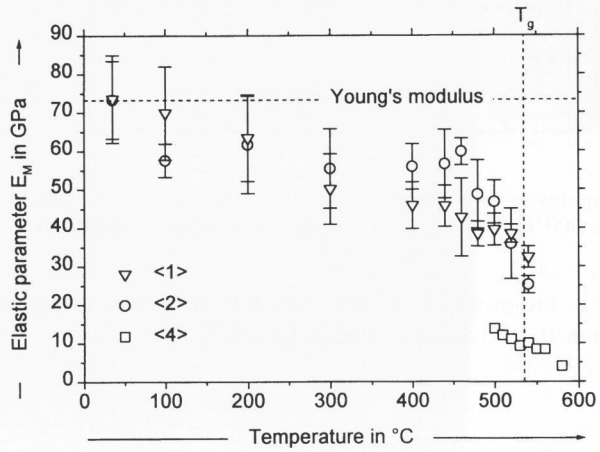

Figure 7. The elastic parameter E_M of the Maxwell model of Vickers indentation experiments (<1>, Γ_v = 1.2) and spherical indentation experiments (<2>, Γ_s = 4.2) analysed by equations (9) and (11) and cylinder compression experiments (<4>) analysed by equations (3) and (4) as a function of temperature. The horizontal dashed line stands for the Young's modulus for orientation.

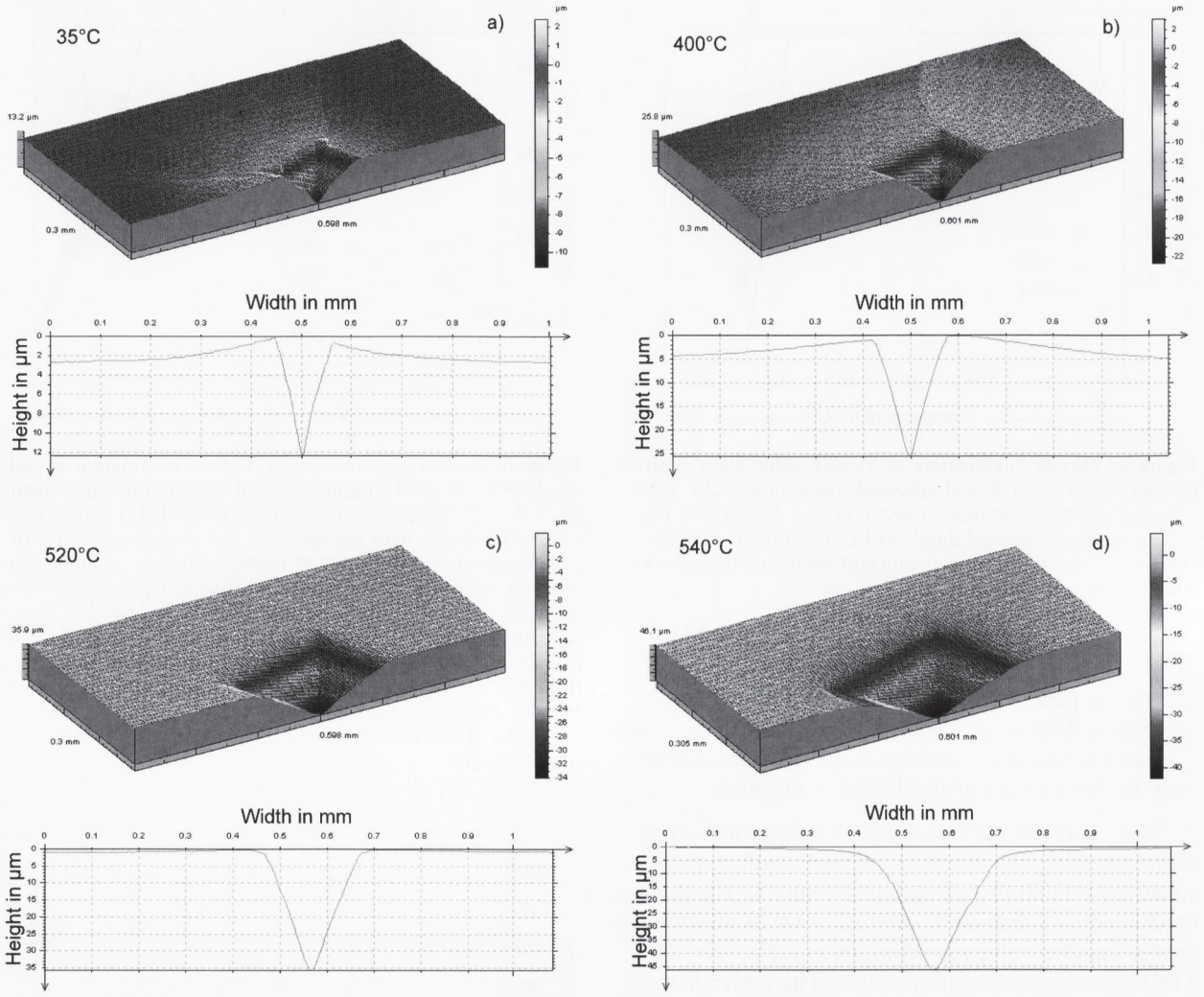

Figures 8a to d. Profile records (top) and single scan lines (bottom) of indents carried out with a Vickers indenter at 35 °C (figure a), 400 °C (figure b), 520 °C (figure c) and 540 °C (figure d).

is in the order of 10^{16} Pa s which is many times smaller than the values suggested in [3 and 4].

4.3 Elastic parameter E_M

In figure 7 the results of the nonlinear least square fit procedure for the elastic parameter E_M are shown for the indentation experiments with Vickers and spherical indenter, respectively, and for the uniaxial cylinder compression experiments of [6]. The very good agreement of the values for the parameters of indentation experiments and the Young's modulus at RT is caused by the calculation procedure for the pre-factor Γ. The quality of the temperature-dependence is in disagreement with results of [16] determined by the flexure pendulum method. There the modulus is approximately constant in the range from RT to T_g. Only just from the vicinity of T_g to higher temperatures the modulus decreases rapidly. The difference between the values of indentation experiments (<1>, <2>) and the cylinder compression experiments (<4>) near T_g is noticeable. But the neglect of the temperature-dependence of the Poisson ratio at the rheological analysis of the indentation experiments is worth mentioning once more, whereas the Poisson ratio is without influence on the calculation of E_M for cylinder compression experiments [6]. Furthermore the real contact areas during indentation experiments at the different temperatures are not known exactly so far. Therefore the real stress behaviour under the indenter is unknown. This problem could be solved by the topographical investigation of the indents. First results are shown in 4.4. The applicability of the "single" Maxwell model to describe the material behaviour during deformation experiments below RT with respect to the results of the modulus calculation will be the subject for future work.

4.4 Topographical investigations of the Vickers indents

Interesting results of the Vickers indentation experiments follow from the profile records on the indents per-

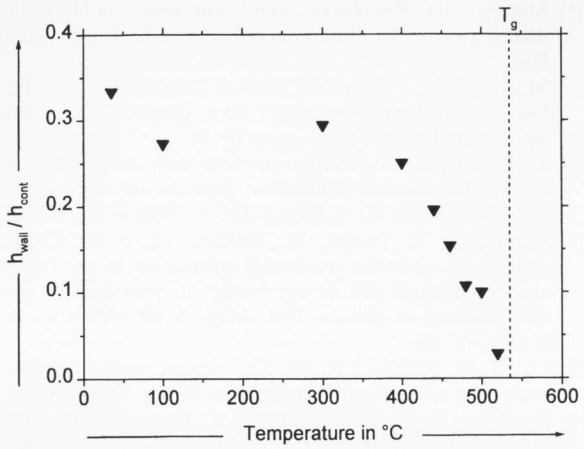

Figure 9. The relation h_{wall}/h_{cont} of the height of the wall h_{wall} and the contact depth h_{cont} as rough results of first topographical investigation of the indents versus temperature.

formed at different typical temperatures (see figures 8a to d) in analogy to the spherical indents in [6]. At RT (35 °C, see figure 8a) as expected permanent cracks at the corners of the indent become visible. But the single scan line parallel with the edge and over the centre of the indent shows the piling-up effect. The height of the wall is about $h_{wall} \approx 3$ µm and the ratio $h_{wall}/h_{cont} \approx 0.3$, where h_{cont} is the distance from the sample surface to the deepest point of the indent. At 400 °C (figure 8b) cracks are also detectable at the corners of the indent. The height of the wall is about $h_{wall} \approx 5$ µm and it is $h_{wall}/h_{cont} \approx 0.25$. At 520 °C (below $T_g = 535$ °C, figure 8c) the indent is without cracks. The height of the wall $h_{wall} \approx 1$ µm yields $h_{wall}/h_{cont} \approx 0.03$. At 540 °C (above T_g, figure 8d) the sinking-in effect is clearly detectable. That means the transition from piling-up to sinking-in occurs in the temperature range from 520 °C to 540 °C. This is the same range as of the corresponding transition in the spherical indentation tests [6]. It is a reasonable supposition that this transition takes place at $T_g = 535$ °C, but systematic investigations are necessary for validated propositions. In figure 9 an analysis of the ration h_{wall}/h_{cont} is shown for a topographical investigation of a single indent per temperature. The extrapolation from RT to T_g points to $h_{wall}/h_{cont} = 0$. That would mean at T_g the complete unloaded permanent indentation depth is equal to the contact depth.

5. Summary and conclusions

The temperature-dependence of the rheological parameters of commercial sheet glass in the temperature range from RT (35 °C) to 540 °C ($T_g = 535$ °C) was investigated by indentation methods with Vickers and spherical indenters, respectively (see also [6]). The analysis of the corresponding hardness numbers HM and H_S (see figure 3) shows the expected decrease of the hardness with increasing temperature. Furthermore, it is visible that the Vickers indentation indicates higher contact stresses than the spherical indentation. In this sense, the smaller values for the viscosity parameter of the rheological analysis of the Vickers indentation in tendency are plausible with respect to the hypothesis which supposes decreasing viscosity with increasing stress. The consistent rheological analysis with the Maxwell model used for both loading and relaxation resulted in viscosity parameters in good accordance with the results of measurements according to conventional viscometer in a temperature range near T_g [6]. The indentation experiments with Vickers and spherical indenters, respectively, have closed the gap for viscosity values from RT to 500 °C (see figure 6). These values show a good correlation to the independent nanoindentation experiments analysed by the same rheological principles. The examination of the temperature-dependence of the viscosity parameters yields an important result of this work. Under the special conditions of very high pressures during indentation experiments, the viscosity values of sheet glass at room temperature are smaller ($\eta < 10^{16}$ Pa s) for experiments analysed by the simple Maxwell model. The elastic parameter E_M of the Maxwell model shows the expected decrease with increasing temperature (see figure 7).

The topographical investigation reveals the deformation conditions of the sample surface around the indent after unloading. The situation is clearly dependent on the temperature. A first rough result of the analysis of the heights of the walls is that the transition from piling-up to sinking-in occurs directly at the transformation temperature in Vickers indentation experiments.

6. List of symbols

A, B, T_0	constants of the Vogel-Fulcher-Tammann equation (12)
C_G	numeric constant of a pyramidal indenter
c	area constant of a pyramidal indenter
E	elastic modulus
E^*	reduced elastic modulus
E_H	elastic parameter of a single Hookean element of the Zener-Maxwell model
E_M	elastic parameter of a Hookean element of the Maxwell model
F	loading force
F_f	loading force at $t = t_f$
F_{max}	maximum load
HM	Martens hardness
H_s	hardness of a spherical indentation according to equation (11)
h	indentation depth
h_{cont}	distance from the sample surface to the deepest point of an indent (contact depth) after unloading
h_{el}	elastic part of the indentation depth
h_{wall}	height of the wall around an indent
h_f	indentation depth at $t = t_f$
$\dot{h}$	indentation rate ($= dh/dt$)
$\dot{h}_c$	constant indentation rate
m_v	geometric constant of the deformation process with a Vickers indenter
R	radius of a spherical indenter
t	time
t_f	duration time of the loading process

T	temperature
T_g	transformation temperature
Γ	material constant
Γ_s	pre-factor of the solution $F(t)$ for deformation by a spherical indenter
Γ_v	pre-factor of the solution $F(t)$ for deformation by a Vickers indenter
ε	strain
ε_f	strain at $t = t_f$
$\dot{\varepsilon}$	strain rate ($= d\varepsilon/dt$)
$\dot{\varepsilon}_c$	constant strain rate
η	viscosity
ν	Poisson ratio
τ	Maxwell relaxation time
σ	stress
σ_f	stress at $t = t_f$
σ_∞	stress at $t \rightarrow \infty$
$\dot{\sigma}$	stress rate ($= d\sigma/dt$)
$\Psi(t)$	viscoelastic function

*

The authors thank the Deutsche Forschungsgemeinschaft, Bonn-Bad Godesberg, (project no. Gr. 1482/1-2) for sponsoring parts of this work.

7. References

[1] Enders, S.: Untersuchungen der mechanischen Eigenschaften von spröden Schicht- und Kompaktsystemen durch Deformation kleiner Volumina. Univ. Halle, Diss. 2000.
[2] Tammann, G.: Der Glaszustand. Leipzig: Voss, 1933.
[3] Frischat, G. H.: Glas – Struktur und Eigenschaften. In: Lohmeyer S. et al. (eds.): Werkstoff Glas I. 2nd. ed. Ehningen: expert, 1987. p. 47–67.
[4] Macosco, C. W.: Rheology – principles, measurements and applications. New York et al.: VCH, 1994.
[5] Meinhard, H.: Rheologische Untersuchungen zu Härteeindruckexperimenten im Nanometerbereich. Univ. Halle, Diss. 1999.
[6] Meinhard, H.; Fränzel, W.; Grau, P.: Viscosity of glass below the transformation temperature. Glastech. Ber. Glass Sci. Technol. **74** (2001) no. 1, p. 6–16.
[7] Sneddon, I. N.: The relation between load and penetration in the axisymmetric Boussinesq problem for a punch of arbitrary profile. Int. J. Engng. Sci. **3** (1965) p. 47–57.
[8] Murakami, Y.; Tanaka, K.; Itokazu, M. et al.: Elastic analysis of triangular pyramidal indentation by the finite-element method and its application to nano-indentation measurement of glasses. Phil. Mag. A **69** (1994) no. 6, p. 1131–1153.
[9] Lee, E. H.; Radok, J. R. M.: The contact problem for viscoelastic bodies. J. appl. Mech. **27** (1960) p. 438–444.
[10] Brückner, R.; Yue, Y.; Deubener, J.: Progress in the rheology of glass melts – A survey. Glastech. Ber. Glass Sci. Technol. **70** (1997) no. 9, p. 261–271.
[11] Wilde, H.-R.; Wehrstedt, A.: Martens Hardness – an international accepted designation for "Hardness under Test Force". Mat.-wiss. u. Werkstofftech. **31** (2000) no. 10, p. 937–940.
[12] Brückner, R.; Yue, Y.; Habeck, A.: Determination of the rheological properties of high-viscous glass melts by the cylinder compression method. Glastech. Ber. Glass Sci. Technol. **67** (1994) no. 5, p. 114–129.
[13] Vogel, H.: Das Temperaturabhängigkeitsgesetz der Viskosität von Flüssigkeiten. Physik. Z. **22** (1921) p. 645–646.
[14] Fulcher, G. S.: Analysis of recent measurements of the viscosity of glasses. J. Am. Ceram. Soc. **8** (1925) p. 339–355; 789–794.
[15] Tammann, G.; Hesse, W.: Die Abhängigkeit der Viskosität von der Temperatur bei unterkühlten Flüssigkeiten. Z. anorg. allg. Chem. **156** (1926) p. 245–257.
[16] Bark-Zollmann, S.; Kluge, G.; Heide, K.: Experimental investigations of the internal friction of optical and technical glasses with a flexure pendulum equipment. Glastech. Ber. Glass Sci. Technol. **71** (1998) no. 3, p. 57–66.

11/1201P004

Address of the authors:

H. Meinhard, W. Fränzel, P. Grau
Martin-Luther-Universität Halle-Wittenberg
Fachbereich Physik
Friedemann-Bach-Platz 6
D-06108 Halle (Saale)